ACS Macro Letters

pubs.acs.org/macroletters Letter

# Alternating Gyroid in Block Polymer Blends

So Jung Park, Frank S. Bates,* and Kevin D. Dorfman*

Cite This: ACS Macro Lett. 2022, 11, 643−650 Read Online

ACCESS | Metrics & More | Article Recommendations | Supporting Information

**ABSTRACT:** Alternating gyroid is a lower symmetry variant of the double gyroid morphology, where the left-handed and right-handed chiral networks are physically distinct. This structure is of particular interest for photonic applications owing to predictions of a complete photonic band gap subject to the requirement of a large dielectric contrast between the individual networks and sufficient optical matching between one of the networks and the matrix. We provide evidence, via self-consistent field theory (SCFT), that stoichiometric blends of double-gyroid-forming AB and BC diblock copolymers with relatively immiscible A and C blocks should form an alternating gyroid morphology with complementary three-dimensional A and C networks that have a free energy that is nearly degenerate with two phase-separated double gyroid states. Solvent casting offers the potential for trapping this binary mixture of diblock copolymers in this metastable alternating gyroid phase. Theory further predicts that the addition of a minuscule amount (<1%) of ABC triblock terpolymer will open an alternating gyroid stability window in the resulting ternary-phase diagram. The surfactant-like stabilization produced by the triblock is relatively insensitive to its exact composition provided the B-block forms a sufficiently long bridge between the A-rich and C-rich networks. This blending strategy provides significant synthetic and material processing advantages compared to prevailing methods to produce an alternating gyroid phase in block polymers.

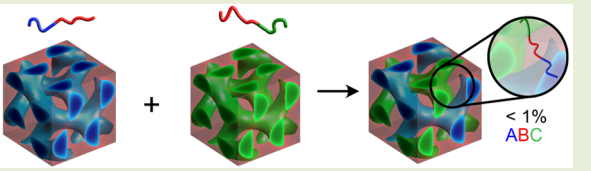




Block polymer self-assembly offers unparalleled opportunities for bottom-up design of nanostructured materials containing 3D continuous and triply periodic nanodomains, targeting applications in myriad areas including catalysis, photonics, membrane technology, and lithography.[1−6] Various network phases have been documented experimentally and theoretically, characterized by 3-fold (double and alternating gyroid, and the single net $O^{70}$), 4-fold (double diamond), or 6-fold (plumber's nightmare) connecting units (see Figure 1).[7−24] Among these network morphologies the alternating gyroid structure is especially appealing, in part because $G^A$ offers the possibility to fabricate materials with a complete photonic band gap.[25−27] According to the computational work by Lequieu et al.,[28] based on a combination of SCFT and photonic band structure calculations, a complete photonic band gap for $G^A$ requires a large refractive index contrast between the individual networks and sufficient optical matching between one of the networks and the matrix. They investigated the design of ABC bottlebrush block polymers, which result in complete photonic bandgap structures, and demonstrated a strategy for achieving complete photonic band gaps with asymmetric networks.

While strategically designed ABC triblocks will form $G^A$,[10,11,16−18] this approach carries several liabilities. First, the $G^A$ phase has been identified only in a very limited portion of an expansive molecular parameter space (three Flory−Huggins $\chi_{ij}$ parameters, two independent composition variables, and the overall molecular weight).[10,11,16,17] Second, access to this morphology is restricted to a small set of synthetically tractable polymer blocks[10,11,16,18] Moreover, establishing the precise conditions for $G^A$ formation would require extensive synthesis and characterization of numerous ABC polymers. Various anticipated applications of $G^A$, such as photonic crystals,[25−27,29,30] also will require removing one of the two networks and backfilling with a metal to create single-gyroid-structured nanomaterials,[31−33] for example, by extraction using a selective solvent,[34] which is not possible with single-component ABC triblocks, although one block could be removed by chemical etching.[35,36]

In this study we investigate the feasibility of preparing $G^A$ materials through diblock blending (Figure 2). Virtually all AB diblock copolymers will self-assemble into the G morphology within two narrow composition windows located between the lamellar (LAM) and hexagonally packed cylindrical (HEX) domain portions of the phase portrait defined by $\chi N$ and $f_A$, where $N$ is the overall degree of polymerization and $f_A$ is the volume fraction of block A. SCFT and numerous experiments show that in the strong segregation limit ($\chi N > 30$) these G windows are about 0.02−0.03 wide in $f_A$.[37−39] While this may appear to be prohibitively narrow, in practice two diblocks with compositions close to the G channel, one HEX and one LAM, can be blended to obtain the G morphology.[40] Intuitively, blending two different G-forming diblocks, AB and BC, where

Received: February 19, 2022
Accepted: April 18, 2022





https://doi.org/10.1021/acsmacrolett.2c00115
ACS Macro Lett. 2022, 11, 643−650

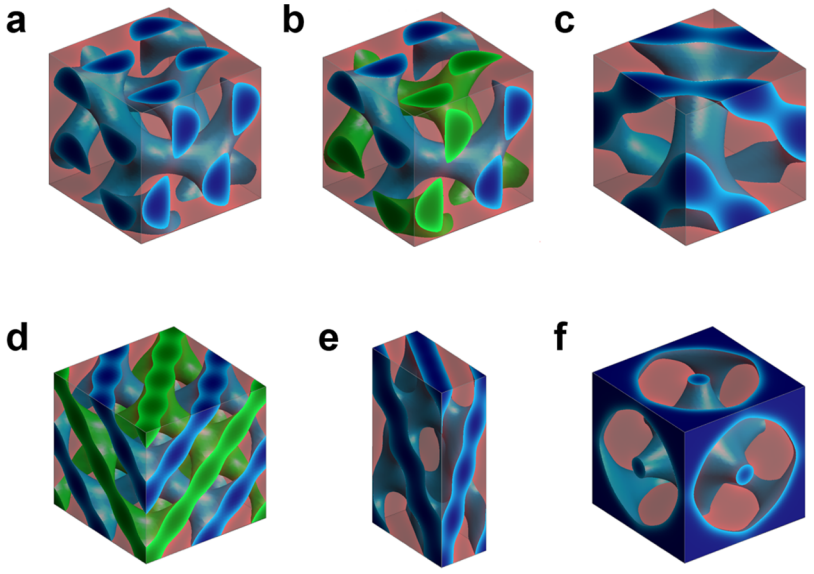


**Figure 1.** Various network phases observed or predicted in block polymers: (a) double gyroid (G), (b) alternating gyroid ($G^A$), (c) double diamond (D), (d) alternating diamond ($D^A$), (e) *Fddd* ($O^{70}$), and (f) plumber's nightmare phases.

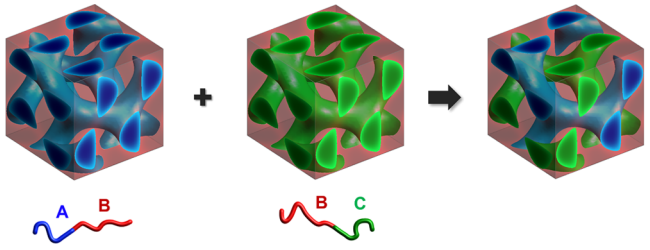


**Figure 2.** Schematics illustrating the strategy of blending AB and BC diblock copolymers that form a double gyroid (G) in the neat melt state to produce an alternating gyroid ($G^A$) structure consisting of two separate interwoven A and C networks, transforming the $Ia\bar{3}d$ symmetry to $I4_132$.

$\chi_{AB} \approx \chi_{BC} \leq \chi_{AC}$, holds the potential for generating the $G^A$ morphology, as illustrated in Figure 2, provided that $G^A$ can be stabilized against macrophase separation into AB-rich and BC-rich double gyroid phases. This approach has significant advantages over the use of ABC triblocks.[10,11,16,18] Many different combinations of blocks can be anticipated, relaxing most of the constraints associated with the triblock, and the block chemistries can be designed to enable removal of one of the networks using a selective solvent to provide the requisite dielectric contrast for photonic applications.

While the phase behaviors of binary blends of AB and BC diblock copolymers have been investigated in other contexts,[2,41−57] surprisingly, the stability of the $G^A$ phase has not been explored yet. To this end, we employed both canonical and grand canonical ensemble SCFT, which provide excellent frameworks for understanding the phase behavior of multicomponent polymeric systems,[58,59] to examine the phase behavior of both incompressible binary blends of AB and BC diblock copolymers and ternary mixtures that included a minor amount of ABC triblock copolymer. Our results indicate that

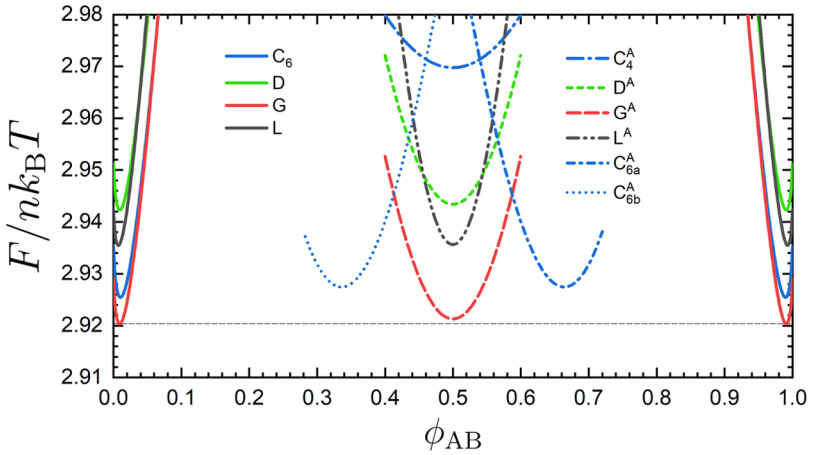


**Figure 3.** Free energy per diblock chain in binary blends of G-forming AB/BC diblocks ($f_A = f_C = 0.357$, $\chi_{AB}N = \chi_{BC}N = 20$, and $\chi_{AC}N = 35$) as a function of AB diblock volume fraction $\phi_{AB}$ for various alternating phases ($C_4^A$, $D^A$, $G^A$, $L^A$, $C_{6a}^A$, and $C_{6b}^A$) and AB- and BC-rich phases ($C_6$, D, G, and L). The $C_{6a}^A$ and $C_{6b}^A$ phases are hexagonally packed alternating cylinder phases with A and B majority cylinders, respectively. The dashed gray tie-line connects the minimums of the AB- and BC-rich G free energy curves. The segment distributions in one example of the AB-rich lamellar phases are provided in Figure S7.



https://doi.org/10.1021/acsmacrolett.2c00115
ACS Macro Lett. 2022, 11, 643−650

the free energies of a blended $G^A$ phase and macroscopically separated G phases are nearly degenerate. Moreover, a minuscule amount of ABC triblock (<1%), when added to the blend, acts like a surfactant, stabilizing the combination of complementary left- and right-handed chiral A and C networks in $G^A$ as the equilibrium state.

The state space for the ternary AB/BC/ABC mixture is very large and anticipated to exhibit a rich phase behavior, including a region of alternating gyroid. For the purposes of this initial communication, we restrict our attention to AB and BC diblocks with minority block degrees of polymerization $N_A = N_C$ and a common value of $N_B$ such that $N = N_A + N_B = N_B + N_C$ is the total degree of polymerization of the diblocks and $f_A = f_C = 0.357$ is the volume fraction of their respective minority blocks. We further selected the Flory–Huggins interaction parameters $\chi_{AB}N = \chi_{BC}N = 20$ and $\chi_{AC}N = 35$. Under these conditions, the pure AB and BC diblocks form the G morphology.[37] The third component, an ABC triblock polymer, has a degree of polymerization $N' = 1.3428\ N$ with equal-sized end blocks, $N'_A = N'_C = 0.4284\ N$, and a center block with $N'_B = 0.486\ N$. In the pure melt state, our SCFT calculations (Figure S9) predict that this ABC triblock forms alternating lamellae ($L^A$) although, as shown below, the precise composition of the triblock is not critical. All polymers were modeled as flexible Gaussian chains with equal statistical segment length, $b$, and segment volume, $\nu$. Free energies of various candidate phases were calculated from the self-consistent mean-field solutions found by numerically solving the modified diffusion equation in SCFT and updating the fields for self-consistency;[58] details regarding the SCFT simulation methods are provided in section S1 of the Supporting Information (SI). For the mixed systems, we considered the following alternating microdomain morphologies: alternating gyroid ($G^A$), alternating diamond ($D^A$), alternating lamellae ($L^A$), square-packed alternating cylinders ($C_4^A$), and hexagonal packed alternating cylinders ($C_6^A$). For the AB or BC diblock-rich phases, we included the well-known hexagonal cylinder ($C_6$), double diamond (D), double gyroid (G), and lamellar (L) phases. All the candidate structures appear in section S2 of the SI.

Figure 3 provides the free energy in the AB/BC binary blend system as a function of the volume fraction of AB diblock polymers, $\phi_{AB}$, for the different candidate phases. The free energy curves are symmetric in $\phi_{AB}$ around $\phi_{AB} = 0.5$ due to the structural equivalence of the AB and BC diblocks. Both micro- and macrophase separation can occur in these two-component mixtures, in contrast to the behavior of single-component block polymers, which cannot simultaneously form multiple coexisting microphase separated states.[43−45,47,48] By design, the minority A and C blocks are thermodynamically incompatible, which enforces microphase separation into discrete domains, separated by a matrix of common B blocks, in the various alternating phases associated with the binary mixtures.

The results in Figure 3 show that mixing the two G-forming diblocks leads to a minimum free energy for the $G^A$ phase at $\phi_{AB} = 0.5$ and that this structure clearly outcompetes all the other alternating phases we have considered. However, the compositionally symmetric ($\phi_{AB} = 0.5$) $G^A$ blend has a slightly higher free energy than the G phases composed of nearly pure AB and BC diblock copolymers, indicating that macrophase separation of the two components represents the equilibrium state. We speculate that the nearly degenerate free energy of the $G^A$ phase, relative to the nearly pure AB and BC G phases with the surprisingly small free energy difference ($\approx 10^{-3} nk_BT$), may result in the formation of $G^A$ when a homogeneous solution of the two diblocks is rapidly solvent cast, analogous to the formation of metastable martensite when a mixture of carbon and iron in the form of FCC austenite is rapidly cooled to low temperature. Diffusion limitations will likely inhibit nucleation and growth of macroscopic G domains, whereas the transition to $G^A$ requires no long-range transport of polymer. Moreover, we provide additional free energy calculations corresponding to the G-forming diblocks at lower $\chi_{AB} = \chi_{BC}$ values in Figure S13. The free energy difference between the blended $G^A$ phase and the macroscopically separated G phases decreases with increasing segregation strength ($\chi N$), indicating that solvent casting will be increasingly viable with higher molecular weight polymers. The same free energy plot in Figure 3 with additional candidate phases (core–shell phases and $O^{70}$) is provided in Figure S8, and the results show that the results inferred from Figure 3 are robust to the inclusion of more candidate phases.

To stabilize the $G^A$ phase against macrophase separation, we added small amounts of the ABC triblock polymer with the hypothesis that this additive would act like a surfactant by bridging the A and C domains in the alternating phases. This strategy resembles stabilization of cocontinuous morphologies in homopolymer blends with ABC triblock terpolymers.[60] Figure 4 shows the effect of the ABC triblock volume fraction

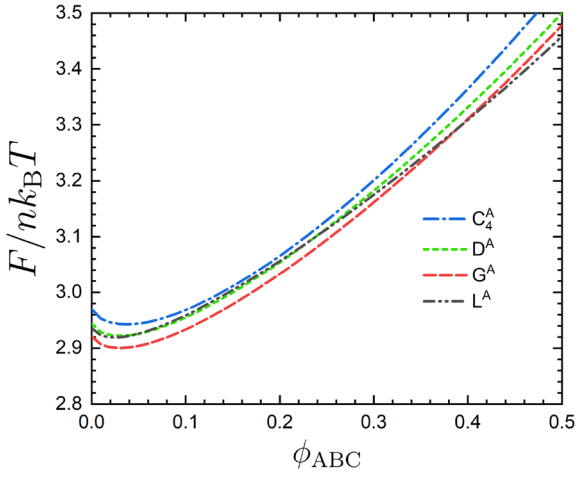


**Figure 4.** Free energy per chain of size $N$ as a function of ABC triblock composition $\phi_{ABC}$ in the ternary blends with the same amount of the AB and BC diblocks ($\phi_{AB} = \phi_{BC} = (1 - \phi_{ABC})/2$). The diblock parameters and interaction strengths are the same as for Figure 3, and the ABC triblock polymer is symmetric ($N'_A = N'_C = 0.4284N$ and $N'_B = 0.486N$), where $N$ is the degree of polymerization of the AB or BC diblock. In the neat melt, this ABC triblock forms the $L^A$ phase.

$\phi_{ABC}$ on the free energy of the alternating phases in blends containing the same amount of AB and BC diblocks ($\phi_{AB} = \phi_{BC}$); a plot showing the full range $0 \le \phi_{ABC} \le 1$ is provided in Figure S9. Small amounts of the ABC triblock reduce the free energy of all the alternating phases, reaching a minimum at $\phi_{ABC} \approx 0.04$; beyond this point, all the free energies increase. For the $G^A$ phase, a considerable reduction in free energy ($\approx 0.02 nk_BT$) is achieved, suggesting that the ternary mixture will stabilize $G^A$ as the equilibrium phase versus the phase separated G states with nearly pure AB and BC diblocks. In


https://doi.org/10.1021/acsmacrolett.2c00115
ACS Macro Lett. 2022, 11, 643−650

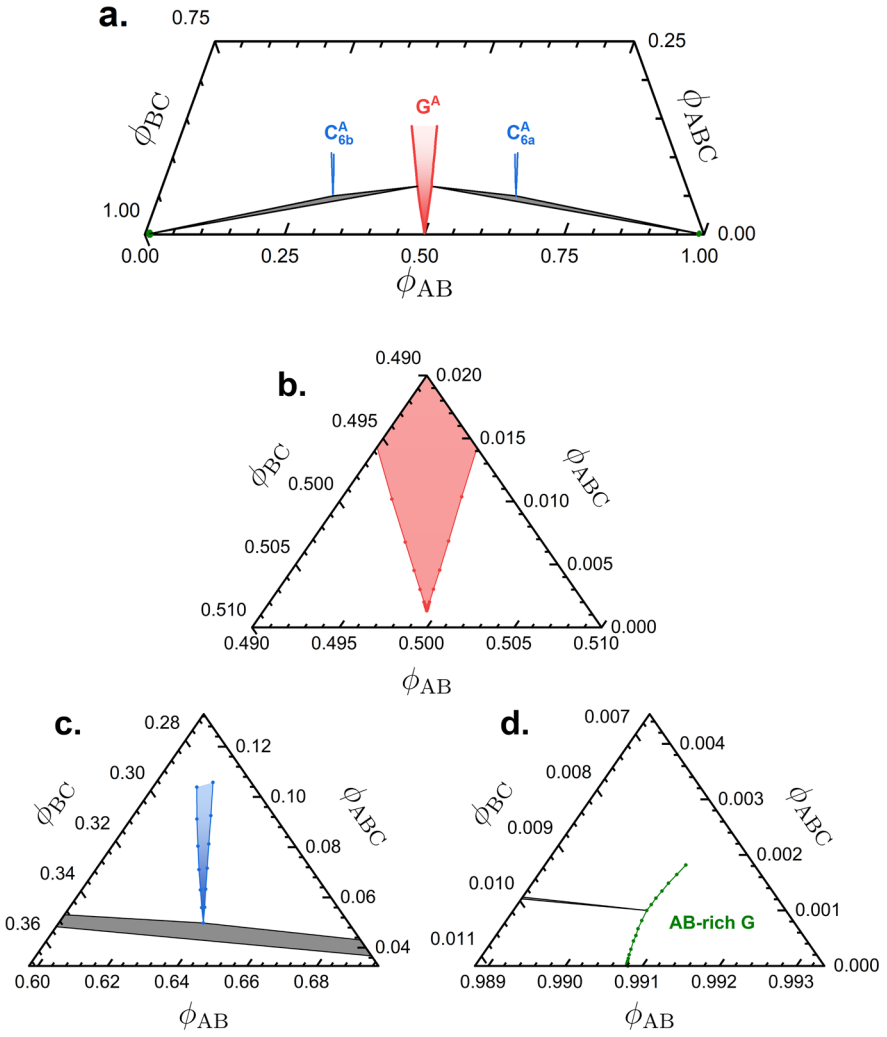


**Figure 5.** Portions of the triangular phase diagram of the AB/BC/ABC ternary blend corresponding to Figure 3 and Figure 4 for (a) the bottom portion of the ternary-phase diagram, (b) the $G^A$ phase window, (c) the stability window of the $C^A_{6a}$ phase with A majority cylinders, and (d) the AB-rich G phase window. The two gray triangles denote the three-phase coexistence windows for the $G^A/C^A_{6b}$/BC-rich G phases and the $G^A/C^A_{6a}$/AB-rich G phases.

order to assess the effect of ABC triblocks on stabilization of the $G^A$ phases in competition with the other possible phases, we plot the free energy surfaces for the $G^A$, $C^A_{6a}$, and AB-rich G phases in Figure S11. These calculations demonstrate that significant decreases in free energy are obtained for both the $G^A$ and $C^A_{6a}$ phases with the addition of a small amount of the ABC triblock, as inferred from the curvature of the free energy surfaces upon moving from the $\phi_{AB}$ edge toward the $\phi_{ABC} = 1$ vertex, which stabilizes these alternating phases. The detailed free energy analysis is provided in the SI section S3.1.

Figure 5 shows the diblock copolymer rich portion of the ternary-phase diagram and the respective stability windows constructed using the grand canonical SCFT solutions; a detailed explanation of the grand canonical SCFT calculations and how the stability and coexistence windows were constructed are provided in SI section S1. Interestingly, the $G^A$ stability window is almost coincident with the $\phi_{ABC} = 0$ edge of the ternary-phase triangle, which means that the minimum amount of ABC triblocks required to open the $G^A$ window is astonishingly small ($\phi_{ABC} = 1.32 \times 10^{-3}$). Here we note that if the diblock blend composition is slightly off the ideal $G^A$ condition (i.e., in the two-phase region separating $G^A$ and G phases), a small amount of double gyroid impurity will be generated in equilibrium with a majority of the $G^A$ phase. We have probed the consequences of varying the block composition in the ABC triblock on the effectiveness of this compatibilizing agent. The results, shown in Figure S15, demonstrate that the minimum amount of triblock required to form the $G^A$ is nearly insensitive to modest variations in the B block and the end block lengths. Therefore, we can safely say that, for a range of ABC compositions, less than 1% of the triblock should suppress macrophase separation and result in a stable $G^A$ phase when added to a symmetric mixture of AB and BC diblocks ($\phi_{AB} = \phi_{BC}$), and the detailed architecture of the ABC triblock is relatively not important in the limit of low $\phi_{ABC}$ acting as a type of surfactant. We also find that the minimum $\phi_{ABC}$ required to open the $G^A$ window becomes smaller as the segregation strength of the double gyroid-forming diblocks increases by comparing Figure 5b to the equivalent results for lower segregation strength in Figure S14. This behavior makes the block copolymer blending strategy appealing for creating large length-scale $G^A$ nanostructures, which is desirable for fabricating photonic band gap, and other, materials.


https://doi.org/10.1021/acsmacrolett.2c00115
ACS Macro Lett. 2022, 11, 643−650

In the extreme limit of a reduced B-block length, i.e., AC diblock polymers, it is intuitive that such additives will not be effective in stabilizing the $G^A$ phase due to unfavorable contacts with the matrix B blocks and a high stretching penalty to bridge the A and C network domains.[61,62] In this limit the ternary blend macroscopically separates into three diblock-rich ordered phases, as shown in Figure S16. Therefore, the middle blocks of ABC triblock polymers should not be too short; as long as the middle block is long enough to bridge the two network domains, macrophase separation is suppressed at low ABC concentrations, independent of the detailed block length ratios since the bridging is insensitive to the minority block length. We expect that the topology of the ternary-phase diagram at high concentrations of the ABC triblock polymers will be sensitive to the architecture of the ABC triblock polymers. For example, an $G^A$-forming ABC triblock polymer would likely result in an $G^A$ window that spans the entire ternary-phase diagram, which will be investigated in a follow-up study. The bottom portion of the ternary-phase diagram is remarkably insensitive to the block composition of the ABC triblock, as shown in Figures S15 and S17, making the blending strategy highly versatile.

While our primary focus in this communication is stabilizing the $G^A$ phase, it has not escaped our attention that there are numerous possible alternating cylinder phases with different arrangements of A and C cylinders, which could make stable states, at different blend compositions, similar to solid solutions in metal alloys, at low values of $\phi_{ABC}$. For notational clarity, let us denote such a solid solution of hexagonally packed cylinders by $C^{SS}_{6a}$, wherein the majority of the cylinders are AB-rich but the AB-rich and BC-rich cylinders are randomly distributed on the hexagonal lattice. Our calculations for the two different $C^{SS}_{6a}$ phases (Figure S6) reveal that they are not as competitive as the $C^{A}_{6a}$ phase (Figure S12) at least for low concentrations of the triblock. In this communication, we focus on the low $\phi_{ABC}$ regime of the phase diagram where the $G^A$ phase is stabilized by the "surfactant-like" action of the ABC triblock. At a moderate to high concentration of triblock, there is the possibility of forming other ordered phases not considered here. Probing the full triangular phase diagram would involve examining all potential phase stability windows. In this context, it would be interesting to investigate the stability of known candidate phases considered in previous publications,[63,64] such as different binary cylinder phases with unequal coordination numbers and sphere−network hybrid morphologies, which could be the subject of future work.

While the cylinder-forming region of the phase diagram is potentially complicated by solid solution-like behavior, the $G^A$ region is simpler. In contrast to the alternating cylinder and alternating sphere phases, which consist of discrete one and zero dimensional domains, respectively, alternating network phases cannot form a solid solution due to the 3D continuous network domain geometry. As a consequence, the $G^A$ stability window is situated at a specific stoichiometric ratio of blend compositions in the ternary-phase diagram, similar to line compounds or phase fields in metal alloy systems.[65] Thus, the ABC triblock polymers act as a type of surfactant, which breaks the symmetry of the G phases in forming the $G^A$ structure.

The AB/BC/ABC ternary system we examined here is one route toward realizing photonic materials in block polymers, but it is not the only possible method suggested by SCFT. Recently, Li and co-workers[66] used SCFT to study a BABAB pentablock copolymer and demonstrated that, through suitable design of the B-block lengths, this system should form a single gyroid network. Indeed, the stability region for single gyroid in BABAB only arises when the middle B block is long enough to provide the bridge, analogous to our requirement for ABC, and the terminal B blocks are able to fill the space to relax chain-stretching penalties. Naturally, a single gyroid is an ideal case of $G^A$ with perfect optical matching between the matrix and the network and could exhibit a complete photonic band gap if sufficient dielectric contrast can be achieved; this likely requires blending with inorganic compounds or extraction of the matrix or a domain and deposition of metal. Another strategy for enhancing optical contrast for the photonic bandgap design is selectively incorporating metal nanoparticles or plasmonic additives in one of the networks to provide sufficient refractive index contrast. Removal of AB or BC based network domains could be accomplished by solvent extraction, a process that is not feasible with single component (e.g., BABAB or pure ABC) materials. Moreover, the synthesis of the pentablock is more involved[67,68] than the simpler approach of solvent casting diblock blends suggested by our work. Even if this processing strategy fails, the results of Figure 5 indicate that $G^A$ can be stabilized by the ABC "surfactant" and that the synthetic precision required for the triblock is not restrictive. There are numerous combinations of polymers that could satisfy the thermodynamic condition $\chi_{AC} \gg \chi_{AB} \approx \chi_{BC}$ invoked in this work, for example, poly(isoprene)-*b*-poly(styrene)−poly(ethylene oxide) (PI−PS−PEO). Selective extraction of one of the diblocks from the $G^A$ morphology could be realized using a solvent that dissolves the A but not the C block. Another strategy is to incorporate a crystallizable A or C block, such as PEO, which also would resist dissolution even with a good solvent.

In summary, we propose that an equilibrium $G^A$ phase can be realized by blending AB and BC diblock polymers with a small amount of ABC triblock polymer, which serves as a symmetry-breaking surfactant. SCFT results reveal that the triblock terpolymer eliminates the tendency for the two diblock copolymers to macrophase separate into nearly pure G phases thus stabilizing the $G^A$ stability window at stoichiometric mixtures of the diblocks. To the best of our knowledge, this is the first study to investigate the feasibility of creating $G^A$ materials through blending diblocks instead of synthesizing $G^A$-forming triblocks or pentablock copolymers. Our work demonstrates that the block copolymer blending strategy, which does not require restrictive triblocks design, can provide an effective and practical route to creating advanced optical materials with complete photonic band gap network nanostructures.

## ■ ASSOCIATED CONTENT

### Supporting Information

The Supporting Information is available free of charge at https://pubs.acs.org/doi/10.1021/acsmacrolett.2c00115.

Details of canonical and grand canonical SCFT calculations including pressure vs chemical potential graphs and phase diagrams; candidate phases and segment density profiles in AB-rich lamellar phase; free energy plots including different candidate phases; 3D free energy surfaces for the $G^A$, $C^{A}_{6a}$, and AB-rich G phases; free energy plots with solid solution phases for hexagonally packed cylinders; free energy plot and $G^A$ phase window with diblocks at lower segregation



https://doi.org/10.1021/acsmacrolett.2c00115
ACS Macro Lett. 2022, 11, 643−650

strength; minimum triblock composition to open the $G^A$ phase window for various triblocks; free energy plot for the $G^A$ phase and three-phase coexistence state in the AB/BC/AC diblock blend; blend composition data for the coexisting phases in the AB/BC/AC diblock blends; ternary-phase diagram with a $G^A$-forming triblock; free energy and phase boundary comparison between different grid sizes (PDF)

## AUTHOR INFORMATION


### Corresponding Authors

**Frank S. Bates** − *Department of Chemical Engineering and Materials Science, University of Minnesota − Twin Cities, Minneapolis, Minnesota 55455, United States;* orcid.org/0000-0003-3977-1278; Email: bates001@umn.edu

**Kevin D. Dorfman** − *Department of Chemical Engineering and Materials Science, University of Minnesota − Twin Cities, Minneapolis, Minnesota 55455, United States;* orcid.org/0000-0003-0065-5157; Email: dorfman@umn.edu

### Author

**So Jung Park** − *Department of Chemical Engineering and Materials Science, University of Minnesota − Twin Cities, Minneapolis, Minnesota 55455, United States;* orcid.org/0000-0002-3003-6501

Complete contact information is available at: https://pubs.acs.org/10.1021/acsmacrolett.2c00115


### Notes

The authors declare no competing financial interest.

## ACKNOWLEDGMENTS

This work was supported primarily by the National Science Foundation primarily through the University of Minnesota Materials Science Research and Engineering Center under Award No. DMR-2011401. We acknowledge the Minnesota Supercomputing Institute (MSI) at the University of Minnesota for providing resources that contributed to the research results reported in this paper.

## REFERENCES


(1) Urbas, A. M.; Maldovan, M.; DeRege, P.; Thomas, E. L. Bicontinuous cubic block copolymer photonic crystals. *Adv. Mater.* **2002**, *14*, 1850−1853.

(2) Tang, C.; Lennon, E. M.; Fredrickson, G. H.; Kramer, E. J.; Hawker, C. J. Evolution of Block Copolymer Lithography to Highly Ordered Square Arrays. *Science* **2008**, *322*, 429−432.

(3) Gin, D. L.; Bara, J. E.; Noble, R. D.; Elliott, B. J. Polymerized lyotropic liquid crystal assemblies for membrane applications. *Macromol. Rapid Commun.* **2008**, *29*, 367−389.

(4) Li, L.; Schulte, L.; Clausen, L. D.; Hansen, K. M.; Jonsson, G. E.; Ndoni, S. Gyroid nanoporous membranes with tunable permeability. *ACS Nano* **2011**, *5*, 7754−7766.

(5) Stefik, M.; Guldin, S.; Vignolini, S.; Wiesner, U.; Steiner, U. Block copolymer self-assembly for nanophotonics. *Chem. Soc. Rev.* **2015**, *44*, 5076−5091.

(6) Hsueh, H. Y.; Yao, C. T.; Ho, R. M. Well-ordered nanohybrids and nanoporous materials from gyroid block copolymer templates. *Chem. Soc. Rev.* **2015**, *44*, 1974−2018.

(7) Hajduk, D. A.; Harper, P. E.; Gruner, S. M.; Honeker, C. C.; Kim, G.; Fetters, L. J.; Kim, G. The Gyroid: A New Equilibrium Morphology in Weakly Segregated Diblock Copolymers. *Macromolecules* **1994**, *27*, 4063−4075.

(8) Matsen, M. W. Phase Behavior of Block Copolymer/Homopolymer Blends. *Macromolecules* **1995**, *28*, 5765−5773.

(9) Matsen, M. W.; Bates, F. S. Origins of Complex Self-Assembly in Block Copolymers. *Macromolecules* **1996**, *29*, 7641−7644.

(10) Epps, T. H.; Cochran, E. W.; Hardy, C. M.; Bailey, T. S.; Waletzko, R. S.; Bates, F. S. Network phases in ABC triblock copolymers. *Macromolecules* **2004**, *37*, 7085−7088.

(11) Epps, T. H.; Cochran, E. W.; Bailey, T. S.; Waletzko, R. S.; Hardy, C. M.; Bates, F. S. Ordered Network Phases in Linear Poly(isoprene-b-styrene-b-ethylene oxide) Triblock Copolymers. *Macromolecules* **2004**, *37*, 8325−8341.

(12) Tyler, C. A.; Morse, D. C. Orthorhombic *Fddd* Network in Triblock and Diblock Copolymer Melts. *Phys. Rev. Lett.* **2005**, *94*, 208302.

(13) Bates, F. S. Network phases in block copolymer melts. *MRS Bull.* **2005**, *30*, 525−532.

(14) Takenaka, M.; Wakada, T.; Akasaka, S.; Nishitsuji, S.; Saijo, K.; Shimizu, H.; Kim, M. I.; Hasegawa, H. Orthorhombic *Fddd* network in diblock copolymer melts. *Macromolecules* **2007**, *40*, 4399−4402.

(15) Martinez-Veracoechea, F. J.; Escobedo, F. A. The Plumber's Nightmare phase in diblock copolymer/homopolymer blends. A self-consistent field theory study. *Macromolecules* **2009**, *42*, 9058−9062.

(16) Meuler, A. J.; Hillmyer, M. A.; Bates, F. S. Ordered network mesostructures in block polymer materials. *Macromolecules* **2009**, *42*, 7221−7250.

(17) Qin, J.; Bates, F. S.; Morse, D. C. Phase Behavior of Nonfrustrated ABC Triblock Copolymers: Weak and Intermediate Segregation. *Macromolecules* **2010**, *43*, 5128−5136.

(18) Kuan, W.-F.; Roy, R.; Rong, L.; Hsiao, B. S.; Epps, T. H. Design and Synthesis of Network-Forming Triblock Copolymers Using Tapered Block Interfaces. *ACS Macro Lett.* **2012**, *1*, 519−523.

(19) Wang, X. B.; Lo, T. Y.; Hsueh, H. Y.; Ho, R. M. Double and single network phases in polystyrene-block-poly(L-lactide) diblock copolymers. *Macromolecules* **2013**, *46*, 2997−3004.

(20) Takagi, H.; Yamamoto, K.; Okamoto, S. Ordered-bicontinuous-double-diamond structure in block copolymer/homopolymer blends. *EPL* **2015**, *110*, 48003.

(21) Chang, C.-Y.; Manesi, G.-M.; Yang, C.-Y.; Hung, Y.-C.; Yang, K.-C.; Chiu, P.-T.; Avgeropoulos, A.; Ho, R.-M. Mesoscale networks and corresponding transitions from self-assembly of block copolymers. *Proc. Natl. Acad. Sci. U.S.A.* **2021**, *118*, No. e2022275118.

(22) Chu, C. Y.; Lin, W. F.; Tsai, J. C.; Lai, C. S.; Lo, S. C.; Chen, H. L.; Hashimoto, T. Order-order transition between equilibrium ordered bicontinuous nanostructures of double diamond and double gyroid in stereoregular block copolymer. *Macromolecules* **2012**, *45*, 2471−2477.

(23) Finnefrock, A. C.; Ulrich, R.; Toombes, G. E.; Gruner, S. M.; Wiesner, U. The Plumber's Nightmare: A New Morphology in Block Copolymer-Ceramic Nanocomposites and Mesoporous Aluminosilicates. *J. Am. Chem. Soc.* **2003**, *125*, 13084−13093.

(24) Toombes, G. E.; Finnefrock, A. C.; Tate, M. W.; Ulrich, R.; Wiesner, U.; Gruner, S. M. A re-evaluation of the morphology of a bicontinuous block copolymer-ceramic material. *Macromolecules* **2007**, *40*, 8974−8982.

(25) Dolan, J. A.; Wilts, B. D.; Vignolini, S.; Baumberg, J. J.; Steiner, U.; Wilkinson, T. D. Optical Properties of Gyroid Structured Materials: From Photonic Crystals to Metamaterials. *Adv. Opt. Mater.* **2015**, *3*, 12−32.

(26) Yoon, J.; Lee, W.; Thomas, E. L. Self-assembly of block copolymers for photonicbandgap materials. *MRS Bull.* **2005**, *30*, 721−726.

(27) Maldovan, M.; Urbas, A. M.; Yufa, N.; Carter, W. C.; Thomas, E. L. Photonic properties of bicontinuous cubic microphases. *Phys. Rev. B* **2002**, *65*, 165123.

(28) Lequieu, J.; Quah, T.; Delaney, K. T.; Fredrickson, G. H. Complete Photonic Band Gaps with Nonfrustrated ABC Bottlebrush Block Polymers. *ACS Macro Lett.* **2020**, *9*, 1074−1080.

(29) Edrington, A. C.; Urbas, A. M.; Derege, P.; Chen, C. X.; Swager, T. M.; Hadjichristidis, N.; Xenidou, M.; Fetters, L. J.;

Joannopoulos, J. D.; Fink, Y.; Thomas, E. L. Polymer-Based Photonic Crystals. *Adv. Mater.* **2001**, *13*, 421−425.
(30) Wang, Z.; Chan, C. L. C.; Zhao, T. H.; Parker, R. M.; Vignolini, S. Recent Advances in Block Copolymer Self-Assembly for the Fabrication of Photonic Films and Pigments. *Adv. Opt. Mater.* **2021**, *9*, 2100519.
(31) Abdollahi, S. N.; Ochoa Martínez, E.; Kilchoer, C.; Kremer, G.; Jaouen, T.; Aebi, P.; Hellmann, T.; Mayer, T.; Gu, Y.; Wiesner, U. B.; Steiner, U.; Wilts, B. D.; Gunkel, I. Carbon-Assisted Stable Silver Nanostructures. *Adv. Mater. Interfaces* **2020**, *7*, 2001227.
(32) Dehmel, R.; Dolan, J. A.; Gu, Y.; Wiesner, U.; Wilkinson, T. D.; Baumberg, J. J.; Steiner, U.; Wilts, B. D.; Gunkel, I. Optical Imaging of Large Gyroid Grains in Block Copolymer Templates by Confined Crystallization. *Macromolecules* **2017**, *50*, 6255−6262.
(33) Hur, K.; Francescato, Y.; Giannini, V.; Maier, S. A.; Hennig, R. G.; Wiesner, U. Three-dimensionally isotropic negative refractive index materials from block copolymer self-assembled chiral gyroid networks. *Angew. Chem., Int. Ed.* **2011**, *50*, 11985−11989.
(34) Yang, K.-C.; Yao, C.-T.; Huang, L.-Y.; Tsai, J.-C.; Hung, W.-S.; Hsueh, H.-Y.; Ho, R.-M. Single gyroid-structured metallic nanoporous spheres fabricated from double gyroid-forming block copolymers via templated electroless plating. *NPG Asia Materials* **2019**, *11*, 9.
(35) Rzayev, J.; Hillmyer, M. A. Nanochannel array plastics with tailored surface chemistry. *J. Am. Chem. Soc.* **2005**, *127*, 13373−13379.
(36) Vignolini, S.; Yufa, N. A.; Cunha, P. S.; Guldin, S.; Rushkin, I.; Stefik, M.; Hur, K.; Wiesner, U.; Baumberg, J. J.; Steiner, U. A 3D optical metamaterial made by self-assembly. *Adv. Mater.* **2012**, *24*, OP23−OP27.
(37) Cochran, E. W.; Garcia-Cervera, C. J.; Fredrickson, G. H. Stability of the gyroid phase in diblock copolymers at strong segregation. *Macromolecules* **2006**, *39*, 2449−2451.
(38) Davidock, D. A.; Hillmyer, M. A.; Lodge, T. P. Persistence of the gyroid morphology at strong segregation in diblock copolymers. *Macromolecules* **2003**, *36*, 4682−4685.
(39) Politakos, N.; Ntoukas, E.; Avgeropoulos, A.; Krikorian, V.; Pate, B. D.; Thomas, E. L.; Hill, R. M. Strongly segregated cubic microdomain morphology consistent with the double gyroid phase in high molecular weight diblock copolymers of polystyrene and poly(dimethylsiloxane). *J. Polym. Sci. B: Polym. Phys.* **2009**, *47*, 2419−2427.
(40) Sakurai, S.; Irie, H.; Umeda, H.; Nomura, S.; Lee, H. H.; Kim, J. K. Gyroid structures and morphological control in binary blends of polystyrene-block-polyisoprene diblock copolymers. *Macromolecules* **1998**, *31*, 336−343.
(41) Ishizu, K.; Omote, A.; Fukutomi, T. Phase separation in binary block copolymer blends. *Polymer* **1990**, *31*, 2135−2140.
(42) Borovinskii, A. L.; Khokhlov, A. R. Microphase separation in a mixture of block copolymers in the strong segregation regime. *Macromolecules* **1998**, *31*, 1180−1187.
(43) Olmsted, P. D.; Hamley, I. W. Lifshitz points in blends of AB and BC diblock copolymers. *Europhys. Lett.* **1999**, *45*, 83−89.
(44) Jeon, H. G.; Hudson, S. D.; Ishida, H.; Smith, S. D. Microphase and Macrophase Transitions in Binary Blends of Diblock Copolymers. *Macromolecules* **1999**, *32*, 1803−1808.
(45) Kimishima, K.; Jinnai, H.; Hashimoto, T. Control of Self-Assembled Structures in Binary Mixtures of A-B Diblock Copolymer and A-C Diblock Copolymer by Changing the Interaction between B and C Block Chains. *Macromolecules* **1999**, *32*, 2585−2596.
(46) Vaidya, N. Y.; Han, C. D. Temperature-composition phase diagrams for binary blends consisting of chemically dissimilar diblock copolymers. *Macromolecules* **2000**, *33*, 3009−3018.
(47) Frielinghaus, H.; Hermsdorf, N.; Sigel, R.; Almdal, K.; Mortensen, K.; Hamley, I. W.; Messé, L.; Corvazier, L.; Ryan, A. J.; van Dusschoten, D.; Wilhelm, M.; Floudas, G.; Fytas, G. Blends of AB/BC Diblock Copolymers with a Large Interaction Parameter $\chi$. *Macromolecules* **2001**, *34*, 4907−4916.
(48) Frielinghaus, H.; Hermsdorf, N.; Almdal, K.; Mortensen, K.; Messé, L.; Corvazier, L.; Fairclough, J. P. A.; Ryan, A. J.; Olmsted, P. D.; Hamley, I. W. Micro- vs. macro-phase separation in binary blends of poly(styrene)-poly(isoprene) and poly(isoprene)-poly(ethylene oxide) diblock copolymers. *Europhys. Lett.* **2001**, *53*, 680−686.
(49) Papadakis, C. M.; Busch, P.; Weidisch, R.; Eckerlebe, H.; Posselt, D. Phase behavior of binary blends of chemically different, symmetric diblock copolymers. *Macromolecules* **2002**, *35*, 9236−9238.
(50) Asari, T.; Matsuo, S.; Takano, A.; Matsushita, Y. Three-phase hierarchical structures from AB/CD diblock copolymer blends with complemental hydrogen bonding interaction. *Macromolecules* **2005**, *38*, 8811−8815.
(51) Mao, H.; Arrechea, P. L.; Bailey, T. S.; Johnson, B. J.; Hillmyer, M. A. Control of pore hydrophilicity in ordered nanoporous polystyrene using an AB/AC block copolymer blending strategy. *Faraday Discuss.* **2005**, *128*, 149−162.
(52) Mao, H.; Hillmyer, M. A. Macroscopic samples of polystyrene with ordered three-dimensional nanochannels. *Soft Matter* **2006**, *2*, 57−59.
(53) Sun, L.; Ginorio, J. E.; Zhu, L.; Sics, I.; Rong, L.; Hsiao, B. S. Phase Transitions and Honeycomb Morphology in an Incompatible Blend of Enantiomeric Polylactide Block Copolymers. *Macromolecules* **2006**, *39*, 8203−8206.
(54) Sun, L.; Zhu, L.; Rong, L.; Hsiao, B. S. Tailor-made onionlike stereocomplex crystals in incompatible, enantiomeric, polylactide-containing block copolymer blends. *Angew. Chem., Int. Ed.* **2006**, *45*, 7373−7376.
(55) Mao, H.; Hillmyer, M. A. Morphological Behavior of Polystyrene -block- Polylactide/Polystyrene -block- Poly(ethylene oxide) Blends. *Macromol. Chem. Phys.* **2008**, *209*, 1647−1656.
(56) Park, W. I.; Kim, Y.; Jeong, J. W.; Kim, K.; Yoo, J.-K.; Hur, Y. H.; Kim, J. M.; Thomas, E. L.; Alexander-Katz, A.; Jung, Y. S. Host-Guest Self-assembly in Block Copolymer Blends. *Sci. Rep.* **2013**, *3*, 3190.
(57) Jung, D. S.; Bang, J.; Park, T. W.; Lee, S. H.; Jung, Y. K.; Byun, M.; Cho, Y. R.; Kim, K. H.; Seong, G. H.; Park, W. I. Pattern formation of metal-oxide hybrid nanostructures via the self-assembly of di-block copolymer blends. *Nanoscale* **2019**, *11*, 18559−18567.
(58) Arora, A.; Qin, J.; Morse, D. C.; Delaney, K. T.; Fredrickson, G. H.; Bates, F. S.; Dorfman, K. D. Broadly Accessible Self-Consistent Field Theory for Block Polymer Materials Discovery. *Macromolecules* **2016**, *49*, 4675−4690.
(59) Shi, A. C. Self-Consistent Field Theory of Inhomogeneous Polymeric Systems. In *Var. Methods Mol. Model.*; Wu, J., Ed.; Springer: Singapore, 2017; pp 155−180.
(60) Fredrickson, G. H.; Bates, F. S. Stabilizing co-continuous polymer blend morphologies with ABC block copolymers. *Eur. Phys. J. B* **1998**, *1*, 71−76.
(61) Xie, Q.; Qiang, Y.; Chen, L.; Xia, Y.; Li, W. Synergistic Effect of Stretched Bridging Block and Released Packing Frustration Leads to Exotic Nanostructures. *ACS Macro Lett.* **2020**, *9*, 980−984.
(62) Xie, Q.; Qiang, Y.; Li, W. Single Gyroid Self-Assembled by Linear BABAB Pentablock Copolymer. *ACS Macro Lett.* **2022**, *11*, 205−209.
(63) Xie, N.; Liu, M.; Deng, H.; Li, W.; Qiu, F.; Shi, A.-C. Macromolecular Metallurgy of Binary Mesocrystals via Designed Multiblock Terpolymers. *J. Am. Chem. Soc.* **2014**, *136*, 2974−2977.
(64) Dong, Q.; Li, W. Effect of Molecular Asymmetry on the Formation of Asymmetric Nanostructures in ABC-Type Block Copolymers. *Macromolecules* **2021**, *54*, 203−213.
(65) de Graef, M.; McHenry, M. E. *Structure of materials: An introduction to crystallography, diffraction, and symmetry*; Cambridge University Press: Cambridge, 2012; Vol. 2.
(66) Xie, Q.; Qiang, Y.; Li, W. Single Gyroid Self-Assembled by Linear BABAB Pentablock Copolymer. *ACS Macro Lett.* **2022**, *11*, 205−209.
(67) Bates, F. S.; Fredrickson, G. H.; Hucul, D.; Hahn, S. F. PCHE-based pentablock copolymers: Evolution of a new plastic. *AIChE J.* **2001**, *47*, 762−765.


https://doi.org/10.1021/acsmacrolett.2c00115
*ACS Macro Lett.* 2022, 11, 643−650

(68) Vigild, M. E.; Chu, C.; Sugiyama, M.; Chaffin, K. A.; Bates, F. S. Influence of shear on the alignment of a lamellae-forming pentablock copolymer. *Macromolecules* **2001**, *34*, 951−964.



https://doi.org/10.1021/acsmacrolett.2c00115
*ACS Macro Lett.* 2022, 11, 643−650